Applied Microbiology and Biotechnology (2020) 104:5259–5272
https://doi.org/10.1007/s00253-020-10580-5

BIOTECHNOLOGICAL PRODUCTS AND PROCESS ENGINEERING

Integrated strain engineering and bioprocessing strategies for high-level bio-based production of 3-hydroxyvalerate in *Escherichia coli*

Dragan Miscevic[1] · Ju-Yi Mao[2] · Teshager Kefale[1,3] · Daryoush Abedi[1,4] · Chih-Ching Huang[2] · Murray Moo-Young[1] · C. Perry Chou[1]

Received: 18 December 2019 / Revised: 15 March 2020 / Accepted: 23 March 2020 / Published online: 14 April 2020

Abstract

As petro-based production generates numerous environmental impacts and their associated technological concerns, bio-based production has been well recognized these days as a modern alternative to manufacture chemical products in a more renewable, environmentally friendly, and sustainable manner. Herein, we report the development of a microbial bioprocess for high-level and potentially economical production of 3-hydroxyvalerate (3-HV), a valuable special chemical with multiple applications in chemical, biopolymer, and pharmaceutical industries, from glycerol, which can be cheaply and renewably refined as a byproduct from biodiesel production. We used our recently derived 3-HV-producing *Escherichia coli* strains for bioreactor characterization under various culture conditions. In the parental strain, 3-HV biosynthesis was limited by the intracellular availability of propionyl-CoA, whose formation was favored by anaerobic conditions, which often compromised cell growth. With appropriate strain engineering, we demonstrated that 3-HV can be effectively produced under both microaerobic (close to anaerobic) and aerobic conditions, which determine the direction of dissimilated carbon flux toward the succinate node in the tricarboxylic acid (TCA) cycle. We first used the Δ*sdhA* single mutant strain, in which the dissimilated carbon flux was primarily directed to the Sleeping beauty mutase (Sbm) pathway (via the reductive TCA branch, with enhanced cell growth under microaerobic conditions, achieving 3.08 g L^{-1} 3-HV in a fed-batch culture. In addition, we used the Δ*sdhA*-Δ*iclR* double mutant strain, in which the dissimilated carbon flux was directed from the TCA cycle to the Sbm pathway via the deregulated glyoxylate shunt, for cultivation under rather aerobic conditions. In addition to demonstrating effective cell growth, this strain has shown impressive 3-HV biosynthesis (up to 10.6 g L^{-1}), equivalent to an overall yield of 18.8% based on consumed glycerol, in aerobic fed-batch culture. This study not only represents one of the most effective bio-based production of 3-HV from structurally unrelated carbons to date, but also highlights the importance of integrated strain engineering and bioprocessing strategies to enhance bio-based production.

Key points

- *TCA cycle engineering was applied to enhance 3-HV biosynthesis in E. coli.*
- *Effects of oxygenic conditions on 3-HV in E. coli biosynthesis were investigated.*
- *Bioreactor characterization of 3-HV biosynthesis in E. coli was performed.*

Keywords *Escherichia coli* · Glyoxylate shunt · Glycerol · 3-hydroxyvalerate · Propionyl-CoA · Sleeping beauty mutase · Strain engineering · TCA cycle

✉ C. Perry Chou
cpchou@uwaterloo.ca

[1] Department of Chemical Engineering, University of Waterloo, 200 University Avenue West, Waterloo, Ontario N2L 3G1, Canada

[2] Department of Bioscience and Biotechnology, National Taiwan Ocean University, Keelung 20224, Taiwan

[3] Department of Biology, University of Waterloo, Waterloo, Ontario N2L 3G1, Canada

[4] Department of Drug & Food Control, School of Pharmacy, Tehran University of Medical Sciences, Tehran, Iran

Introduction

Mounting concerns over finite fossil fuels and their environmental impacts have created growing needs to use renewable and clean carbon sources for the production of chemical compounds. An emerging technology for manufacturing of chemicals involves the use of biological cell factories, such as microorganisms, as biocatalysts for transformation, so called bio-based production or biomanufacturing. While whole-cell biocatalysts have many benefits over conventional chemical catalysts, natural organisms often have a limited metabolic capacity to meet the increasing demands in chemical product variety and quantity. Recent biotechnological advances in synthetic biology, genetic engineering, and metabolic engineering can substantially improve bio-based production (Yaguchi et al. 2018). To date, successful bio-based production includes not only fine chemicals but also commodity chemicals, such as succinate (Mao et al. 2018), lactate (Zhou et al. 2013), lysine (Xu et al. 2014), and polyhydroxyalkanoates (PHAs) (Kaur and Roy 2015; Luo et al. 2014). A major issue limiting bio-based production is the high feedstock cost; therefore, cheap renewable feedstocks are under constant exploration. As a byproduct associated with biodiesel production, refined glycerol can be obtained inexpensively these days (Ciriminna et al. 2014). Moreover, glycerol has been regarded as an effective carbon source for microbial cultivation due to its highly reduced nature, generating approximately twice the number of reducing equivalents upon its degradation compared with traditional fermentable sugars (Murarka et al. 2008; Yazdani and Gonzalez 2007). Hence, glycerol serves as a preferred feedstock for microbial production of several chemicals, such as succinate, 1,3-propanediol, 2,3-butanediol, and PHAs (Zhu et al. 2013).

3-Hydroxyacids are a group of fine chemicals to be used as precursors for making a selection of antibiotics, vitamins, pheromones, and aromatic derivatives (Fonseca et al. 2019; Mori 1981; Nahar et al. 2009; Toshiyuki and Takeshi 1987). Currently, most 3-hydroxyacids are still produced via chemical reactions (Noyori et al. 2004; Spengler and Albericio 2014; Ren et al. 2010) or chemical degradation of PHAs (de Roo et al. 2002). Being more environmentally friendly and sustainable, bio-based production has a potential to replace these chemical processes for 3-hydroxyacid production. It is generally conducted in two ways: i.e., (i) depolymerization of PHAs (Anis et al. 2017; Biernacki et al. 2017) and (ii) direct biosynthesis (Tseng et al. 2010, 2009). Among various 3-hydroxyacids, 3-hydroxybutyrate (3-HB) is the most common one and the monomer of polyhydroxybutyrate (PHB). In general, 3-HB biosynthesis starts with a structural fusion of two acetyl-CoA moieties to form acetoacetyl-CoA, followed by subsequent reduction and CoA removal steps (Fig. 1); and the associated key enzymes, such as acetoacetyl-CoA thiolase (PhaA) and acetoacetyl-CoA reductase (PhaB), exist in many microorganisms that produce PHA (Taroncher-Oldenburg et al. 2000).

3-Hydroxyvalerate (3-HV) is a C5-counterpart of 3-HB and serves as a precursor for several pharmaceutical molecules (Huang et al. 1998). Also, 3-HV can be introduced into the PHB polymeric chain to form a biocopolymer, poly(3-hydroxybutyrate-*co*-3-hydroxyvalerate) (PHBV), which is structurally more ductile, flexible, and tougher than the PHB homopolymer (Lau et al. 2014; Snell and Peoples 2009). While being more bioactive and valuable than 3-HB, 3-HV has various technological and economic challenges in biosynthesis, ultimately limiting its industrial applications. Herein, we report a bioprocess development based on engineered *E. coli* strains recently derived for 3-HV production (with 3-HB being co-produced) from glycerol (Miscevic et al. 2019). Basically, a propanologenic (i.e., 1-propanol-producing) *E. coli* strain with an activated Sleeping beauty mutase (Sbm) operon (i.e., *sbm-ygfD-ygfG-ygfH*) was used as a host. The encoding enzymes (i.e., Sbm, YgfD, YgfG, and YgfH) of the Sbm operon are involved in a metabolic pathway for extended dissimilation of succinate to form propionyl-CoA, and subsequently 1-propanol and propionate as fermentative metabolites (Fig. 1) (Srirangan et al. 2013, 2014). Structurally, 3-HV can be derived via a biosynthetic pathway similar to that of 3-HB (Fig. 1) with one acetyl-CoA moiety being replaced by propionyl-CoA. Note that the use of our propanologenic *E. coli* strains (with the presence of non-native propionyl-CoA) as the production host can eliminate a common but expensive bioprocess requirement, i.e. supplementation of structurally related carbons such as propionate, valerate, 3-hydroxynitrile, and levulinate (Martin and Prather 2009), significantly reducing the 3-HV production cost.

Based on the 3-HV biosynthetic pathway (Fig. 1), high-level 3-HV production potentially relies on the intracellular availability of propionyl-CoA as a key precursor. Though the Sbm pathway was activated in our original propanologenic *E. coli* strain, the intracellular propionyl-CoA level might remain low since the Sbm pathway is not physiologically essential, limiting the biosynthesis of propionyl-CoA-derived compounds. The major objective of this study is to tackle such metabolic limitation. As succinyl-CoA serves as a precursor toward the Sbm pathway, the tricarboxylic acid (TCA) cycle becomes a plausible target for metabolic manipulation. However, since succinyl-CoA is involved in the central metabolism in a complex manner and its formation can be mediated through multiple pathways, manipulation of the carbon flux around this C4-compound can be challenging. In addition, carbon flux channeling from the TCA cycle to the Sbm pathway in *E. coli* appears to be highly sensitive to the oxygenic condition of the culture. Herein, we developed consolidated strain engineering (i.e., manipulation of TCA cycle) and bioprocessing (i.e., regulation of culture aeration) strategies for effective carbon flux direction and, therefore,

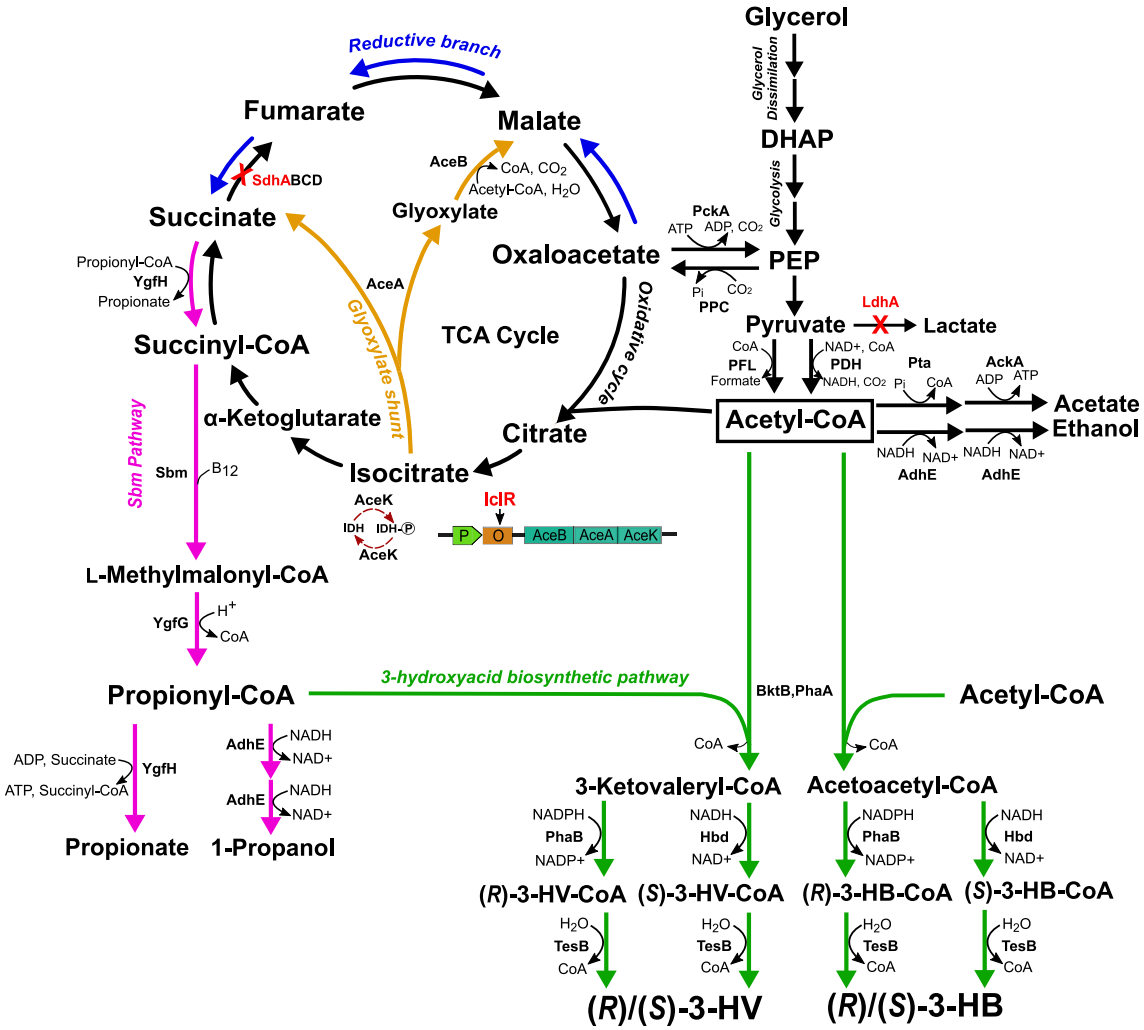

Fig. 1 Schematic representation of natural and engineered pathways in *E. coli* using glycerol as the carbon source. Metabolic pathways outlined: glycerol dissimilation, central metabolism, and oxidative TCA cycle (in black); glyoxylate shunt of TCA cycle (in dark yellow); reductive branch of TCA cycle (in blue); Sbm pathway (in purple); 3-hydroxyacid biosynthetic pathway (in green). Metabolite abbreviations: 3-HB, 3-hydroxybutyrate; 3-HV, 3-hydroxyvalerate; DHAP, dihydroxyacetone phosphate; PEP, phosphoenolpyruvate; (*S*)/(*R*)-3-HB-CoA, (*S*)/(*R*)-3-hydroxybutyryl-CoA; (*S*)/(*R*)-3-HV-CoA, (*S*)/(*R*)-3-hydroxyvaleryl-CoA. Protein abbreviations: AceA, isocitrate lyase; AceB, malate synthase A; AceK, isocitrate dehydrogenase kinase/phosphatase; AckA, acetate kinase; AdhE, aldehyde-alcohol dehydrogenase; BktB, beta-ketothiolase; Hbd, beta-hydroxybutyryl-CoA dehydrogenase; IclR, AceBAK operon repressor; IDH, isocitrate dehydrogenase; IDH-P, isocitrate dehydrogenase-phosphate; LdhA, lactate dehydrogenase A; PckA, phosphoenolpyruvate carboxykinase; PDH, pyruvate dehydrogenase; PFL, pyruvate formate-lyase; PhaA, acetoacetyl-CoA thiolase; PhaB, acetoacetyl-CoA reductase; PK, pyruvate kinase; PPC, phosphoenolpyruvate carboxylase; Pta, phosphotransacetylase; Sbm, methylmalonyl-CoA mutase; SdhABCD, succinate dehydrogenase complex; TesB, acyl-CoA thioesterase II; YgfG, (*R*)-methyl-malonyl-CoA carboxylase; YgfH, propionyl-CoA: succinate CoA-transferase

enhanced 3-HV production, demonstrating potential industrial applicability of the developed bioprocess.

Materials and methods

Bacterial strains and plasmids

Bacterial strains, plasmids, and deoxynucleic acid (DNA) primers used in this study are listed Table 1. Genomic DNA from bacterial cells was isolated using the Blood & Tissue DNA Isolation Kit (Qiagen, Hilden, Germany). Standard recombinant DNA technologies were applied for molecular cloning (Miller 1992). All plasmids were constructed by Gibson enzymatic assembly (Gibson et al. 2009). Phusion HF and *Taq* DNA polymerases were obtained from New England Biolabs (Ipswich, MA, USA). All synthesized oligonucleotides were obtained from Integrated DNA Technologies (Coralville, IA, USA). DNA sequencing was conducted by the Centre for Applied Genomics at the Hospital for Sick Children (Toronto, Canada). *E. coli* BW25113 was the parental strain for derivation of all mutant strains in this study, and

Table 1 *E. coli* strains, plasmids, and oligonucleotides used in this study

Name	Description, relevant genotype or primer sequence (5′ ➔ 3′)	Source
E. coli host strains		
DH5α	F−, *endA1, glnV44, thi-1, recA1, relA1, gyrA96, deoR, nupG φ80d lacZΔacZd ladlacZYA – argF) U169, hsdR17(rK-mK +), λ-*	Lab stock
BW25113	F-, *Δ(araD-araB)567, ΔlacZ4787(::rrnB-3), λ-, rph-1, Δ(rhaD-rhaB)568, hsdR514*	(Datsenko and Wanner 2000)
BWΔ*ldhA*	BW25113 *ldhA* null mutant	(Akawi et al. 2015; Srirangan et al. 2016a; Srirangan et al. 2014)
CPC-Sbm	BWΔ*ldhA*, P*trc::sbm* (i.e., with the FRT-P*trc* cassette replacing the 204-bp upstream of the Sbm operon)	(Akawi et al. 2015)
P3HA31	CPC-Sbm/pTrc-PhaAB and pK- BktB-Hbd-TesB	(Miscevic et al. 2019)
P3HA31Δ*sdhA*	*sdhA* null mutant of P3HA31	(Miscevic et al. 2019)
P3HA31Δ*iclR*	*iclR* null mutant of P3HA31	(Miscevic et al. 2019)
P3HA31Δ*sdhA*Δ*iclR*	*sdhA* and *iclR* null mutant of P3HA31	(Miscevic et al. 2019)
Plasmids		
pTrc99a	ColE1 ori Apr P*trc*	(Amann et al. 1988)
pK184	p15A ori, KmR, P*lac::lacZ*′	(Jobling and Holmes 1990)
pTrc-PhaAB	Derived from pTrc99a, P_{trc}::*phaAB*	Lab stock
pK-BktB-Hbd-TesB	Derived from pK184, P_{lac}::*bktb:hbd:tesB*	Lab stock
Primers		
v-ldhA	GATAACGGAGATCGGGAATGATTAA; GGTTTAAAAGCGTCGATGTCCAGTA	(Akawi et al. 2015)
v-sdhA	CTCTGCGTTCACCAAAGTGT; ACACACCTTCACGGCAGGAG	(Miscevic et al. 2019)
v-iclR	GGTGGAATGAGATCTTGCGA; CCGACACGCTCAACCCAGAT	(Miscevic et al. 2019)
c-frt	AGATTGCAGCATTACACGTCTTGAG; CCAGCTGCATTAATGAATCGGGCCATGGTCCATATGAATATCCTCC	(Srirangan et al. 2014)
c-ptrc	CCGATTCATTAATGCAGCTGG; GGTCTGTTTCCTGTGTGAAATTGTTA	(Srirangan et al. 2016b)
g-phaAB	**CCGGCTCGTATAATGTGTGG**ATGACTGACGTTGTCATCGTATCC; **ATTGTTATCCGCTCACAATT**TCAGCCCATATGCAGGCCGC	Lab stock
g-tesB	**ACAGGAAACAGCTATGAC**ATGAGTCAGGCGCTAAA **GAGCTCGAATTCGTAATCA**TTAATTGTGATTACGCATCAC	Lab stock
g-bktb	**CACAGGAAACAGCTATGACC**ATGACGCGTGAAGTGGTAGT; **TAAACAGACCTCCCTTAAATTTAAT**TCAGATACGCTCGAAGATGG	Lab stock
g-hbd	**TTAAATTTAAGGGAGGTCTGTTTA**ATGAAAAAGGTATGTGTTATAGG; **TAACAAAGCTGCCGCAG**TTATTTTGAATAATCGTAGAAACCTTT	Lab stock
g-pTrc-phaAB	GCGGCCTGCATATGGGCTGA**TGGAATTCGAGCTCGGTACC**; ACGATGACAACGTCAGTCAT**GTCTGTTTCCTGTGTGAAATTGTTAT CCG**	Lab stock
g-pK-bktB-hbd-tesB	**GGTGATGCGTAATCACAATTAA**TGATTACGAATTCGAGCTCGG; **TACCACTTCACGCGTCAT**GGTCATAGCTGTTTCCTGTGTGAA	Lab stock

E. coli DH5α was used as a host for molecular cloning. It should be emphasized that the *ldhA* gene (encoding lactate dehydrogenase) was previously inactivated in BW25113, generating BWΔ*ldhA* (Srirangan et al. 2014). Activation of the genomic Sbm operon in BWΔ*ldhA* to generate propanologenic *E. coli* CPC-Sbm was described previously (Srirangan et al. 2014).

Implementation of 3-hydroxyacid-biosynthetic pathway in propanologenic *E. coli* to form 3-HV-producing strains was recently reported (Miscevic et al. 2019). Briefly, the *phaAB* operon was PCR-amplified using the primer set g-phaAB and the genomic DNA of wild-type *Cupriavidus necator* ATCC 43291 as the template. The amplified operon was Gibson-assembled (note that "assembled" is used for subsequent appearance) with the PCR-linearized pTrc99a using the primer set g-pTrc-phaAB to generate pTrc-PhaAB. All genes inserted into pTrc99a vector were under the control of the P_{trc} promoter. Plasmid pK-BktB-Hbd-TesB was previously constructed in our lab by PCR-amplifying *bktB* from *C. necator* ATCC 43291, *hbd* from *Clostridium acetobutylicum* ATCC 824, and

tesB from *E. coli* BW 25141 using the corresponding primer sets (i.e., g-bktB, g-hbd, and g-tesB), followed by assembling all three PCR-amplified fragments with the PCR-linearized pK184 using the primer set g-pK-bktB-hbd-tesB. All genes inserted into pK184 vector were under the control of the P_{lac} promoter.

Gene knockouts were introduced into *E. coli* recipient strains by P1 phage transduction (Miller 1992) using the appropriate Keio Collection strains (The Coli Genetic Stock Center, Yale University, New Haven, CT, USA) as donors (Baba et al. 2006). To eliminate the co-transduced FRT-Kn^R-FRT cassette, the transductants were transformed with pCP20 (Cherepanov and Wackernagel 1995), a temperature-sensitive plasmid expressing a flippase (Flp) recombinase. Upon Flp-mediated excision of the Kn^R cassette, a single Flp recognition site (FRT "scar site") was generated. Plasmid pCP20 was then cured by growing cells at 42 °C. The genotypes of derived knockout strains were confirmed by colony polymerase chain reaction (PCR) using the appropriate verification primer sets listed in Table 1.

Media and bacterial cell cultivation

All medium components were obtained from Sigma-Aldrich Co. (St Louis, MO, USA) except glucose, yeast extract, and tryptone which were obtained from BD Diagnostic Systems (Franklin Lakes, NJ, USA). The media were supplemented with antibiotics as required: 25 μg mL^{-1} kanamycin and 50 μg mL^{-1} ampicillin. *E. coli* strains, stored as glycerol stocks at − 80 °C, were streaked on lysogeny broth (LB) agar plates with appropriate antibiotics and incubated at 37 °C for 14–16 h. Single colonies were picked from LB plates to inoculate 30-mL super broth (SB) medium (32 g L^{-1} tryptone, 20 g L^{-1} yeast extract, and 5 g L^{-1} NaCl) with appropriate antibiotics in 125-mL conical flasks. Overnight cultures were shaken at 37 °C and 280 rpm in a rotary shaker (New Brunswick Scientific, NJ, USA) and used as seed cultures to inoculate 220 mL SB media at 1% (v/v) with appropriate antibiotics in 1-L conical flasks. This second seed culture was shaken at 37 °C and 280 rpm for 14–16 h. Cells were then harvested by centrifugation at 9000×*g* and 20 °C for 10 min and resuspended in 50 mL fresh LB media. The suspended culture was used to inoculate a 1-L stirred tank bioreactor (containing two Rushton radial flow disks as impellers) (CelliGen 115, Eppendorf AG, Hamburg, Germany) at 30 °C and 430 rpm. The semi-defined production medium in the batch bioreactor contained 30 g L^{-1} glycerol, 0.23 g L^{-1} K_2HPO_4, 0.51 g L^{-1} NH_4Cl, 49.8 mg L^{-1} $MgCl_2$, 48.1 mg L^{-1} K_2SO_4, 1.52 mg L^{-1} $FeSO_4$, 0.055 mg L^{-1} $CaCl_2$, 2.93 g L^{-1} NaCl, 0.72 g L^{-1} tricine, 10 g L^{-1} yeast extract, 10 mM $NaHCO_3$, 0.2 μM cyanocobalamin (vitamin B_{12}) and 1000th dilution (i.e., 1 mL L^{-1}) trace elements (2.86 g L^{-1} H_3BO_3, 1.81 g L^{-1} $MnCl_2$•$4H_2O$, 0.222 g L^{-1} $ZnSO_4$•$7H_2O$, 0.39 g L^{-1} Na_2MoO_4•$2H_2O$, 79 μg L^{-1} $CuSO_4$•$5H_2O$, 49.4 μg L^{-1} $Co(NO_3)_2$•$6H_2O$) (Neidhardt et al. 1974), appropriate antibiotics, and supplemented with 0.1 mM isopropyl β-D-1-thiogalactopyranoside (IPTG). For fed-batch cultivation, the production strain was first cultivated in a batch mode, as described above, followed by three feeding phases, in each of which ~ 15 g L^{-1} glycerol was supplemented for extended cultivation until complete glycerol dissimilation. Microaerobic and semiaerobic conditions were maintained by purging air into the headspace and bulk culture, respectively, at 0.1 vvm, designated as aeration level I (AL-I) and AL-II. Aerobic conditions were maintained by sparging air into the bulk culture at 1 vvm (AL-III) or 2–4 vvm (AL-IV). The pH of the production culture was maintained at 7.0 ± 0.1 with 30% (v/v) NH_4OH and 15% (v/v) H_3PO_4.

Analysis

Culture samples were appropriately diluted with 0.15 M saline solution for measuring cell density in OD_{600} using a spectrophotometer (DU520, Beckman Coulter, Fullerton, CA). Cell-free medium was prepared by centrifugation of the culture sample at 9000×*g* for 5 min, followed by filter sterilization using a 0.2-μm syringe filter. Extracellular metabolites and glycerol were quantified using high-performance liquid chromatography (HPLC) (LC-10AT, Shimadzu, Kyoto, Japan) with a refractive index detector (RID; RID-10A, Shimadzu, Kyoto, Japan) and a chromatographic column (Aminex HPX-87H, Bio-Rad Laboratories, CA, USA). The HPLC column temperature was maintained at 35 °C, and the mobile phase was 5 mM H_2SO_4 (pH 2) running at 0.6 mL min^{-1}. The RID signal was acquired and processed by a data processing unit (Clarity Lite, DataApex, Prague, Czech Republic).

Results

Effects of oxygenic conditions on 3-HV biosynthesis

The propanologenic *E. coli* with an activated Sbm operon, i.e., CPC-Sbm, was used as a host, and a double plasmid system was employed to express key enzymes in the 3-HV biosynthetic pathway (Fig. 1), including (1) PhaA (encoded by *phaA*) and BktB (encoded by *bktB*) for hetero-fusion of propionyl-CoA and acetyl-CoA moieties to 3-ketovaerlyl-CoA, (2) Hbd (encoded by *hbd*) and PhaB (encoded by *phaB*) for reduction of 3-ketovaleryl-CoA to 3-hydroxyvaleryl-CoA (3-HV-CoA), and (3) TesB (encoded by *tesB*) for conversion of 3-HV-CoA to 3-HV. The resulting engineered strain P3HA31 was used as the control strain for

bioreactor cultivation for 3-HV production. Note that these enzymes also have the activity toward their C4 counterpart species in all steps of the engineered pathway (Fig. 1), resulting in the co-production of 3-HB and 3-HV. Several major metabolic pathways are involved for 3-HV biosynthesis in *E. coli*, including those for glycerol dissimilation, TCA cycle, Sbm fermentation, and 3-hydroxyacid biosynthesis (Fig. 1). These metabolic pathways, along with cell growth, can be sensitive to cultivation conditions in different levels. Specifically, the oxygenic condition could critically affect direction of the dissimilated carbon flux from the TCA cycle to the Sbm pathway for 3-HV biosynthesis. To investigate such oxygenic effects, batch cultivation of the control strain P3HA31 in a bioreactor was subject to three levels of aeration, i.e., AL-I, AL-II, and AL-III (from low to high).

The aeration level had major physiological and metabolic effects on P3HA31 (Fig. 2). Under AL-I, glycerol consumption and cell growth were significantly retarded with only 15.8 g L^{-1} glycerol being dissimilated after 39 h and the maximal cell density reaching only 8.0 OD_{600}. On the other hand, glycerol dissimilation was rather effective and complete under both AL-II and AL-III, with the final cell density reaching 17.6 and 18.4 OD_{600}, respectively. The enhanced cell growth appeared to be in line with 3-HB production, i.e., 1.68 g L^{-1} (18.7% yield) under AL-I, 4.92 g L^{-1} (26.1% yield) under AL-II, and 5.21 g L^{-1} (28.1% yield) under AL-III. However, the time profiles of acetate formation, which could potentially reflect cell physiology, were different under these three aeration conditions. There was a significant acetate accumulation toward the end of P3HA31 cultivation under AL-I, suggesting a potential carbon spill at the acetyl-CoA node upon the growth arrest, whereas the secreted acetate was subsequently dissimilated for P3HA31 cultivation under AL-II. However, acetate accumulation reappeared for P3HA31 cultivation under AL-III even though there was no growth arrest. On the other hand, it appears that the level of Sbm fermentation was highly dependent on the oxygenic condition as the production of 3-HV and odd-chain metabolites (i.e., 1-propanol, propionate, and 3-HV) in P3HA31 increased with a reduced oxygen availability. Note that trace amounts of 1-propanol and succinate were even present under AL-I. While the 3-HV titers were rather similar for P3HA31 cultivations under AL-I and AL-II, the 3-HV yield of the cultivation under AL-I was 2.3-fold that under AL-II. In addition, the yield of odd-chain metabolites was 28.4% and 7.92% under AL-I and AL-II, respectively. Interestingly, no 3-HV or any odd-chain metabolite was detected under AL-III, implying that the Sbm pathway activity was minimal in P3HA31 under aerobic conditions. The results suggest that, although the Sbm fermentation was favored by anaerobiosis, the associated poor glycerol dissimilation and cell growth could limit the overall cultivation performance for 3-HV production.

Strain engineering for 3-HV biosynthesis under microaerobic conditions

To alleviate ineffective glycerol dissimilation and cell growth in P3HA31 under AL-I, we derived a single-knockout mutant P3HA31Δ*sdhA* in which the oxidative TCA cycle was inactivated (Fig. 3), achieving faster glycerol consumption (31.2 g L^{-1} glycerol dissimilated in 36 h) and higher cell density (12.2 OD_{600}). With these physiological improvements, P3HA31Δ*sdhA* produced nearly 2-fold 3-HV titer with an overall 3-HV yield comparable to P3HA31 under AL-I. Interestingly, cultivation of P3HA31Δ*sdhA* under AL-III led to seriously defective carbon dissimilation (consuming only 6.24 g L^{-1} glycerol after 23 h cultivation), cell growth (final cell density of 7.61 OD_{600}), and metabolite production (no 3-HV and other odd-chain metabolites). The secreted acetate in P3HA31Δ*sdhA* under AL-III accounted for 87% of dissimilated glycerol, which is more than 5-fold that in P3HA31 under the same aeration condition, implying a serious carbon spill associated with the stressful cell physiology. These results suggest that the dissimilated carbon flux was directed from the TCA cycle to the Sbm pathway for 3-HV biosynthesis via the reductive TCA branch under microaerobic conditions, and such carbon flux channeling became more effective upon inactivating the oxidative TCA cycle.

We further explored the 3-HV biosynthetic capacity in P3HA31Δ*sdhA* under AL-I by extending the existing batch culture with three pulse glycerol feedings (i.e., feeding 1–3), each at 15 g L^{-1} (Fig. 4). While there was no cell growth during the three feeding phases, cells continued to consume glycerol to form various metabolites. The 3-HV and odd-chain yields (i.e., combined yields of 3-HV, propionate, and 1-propanol) remained relatively constant (around 5–7%), whereas the 3-HB yield continuously increased (from 10.4 to 31.5%) throughout the entire fed-batch cultivation, achieving final titers of 3.08 g L^{-1} 3-HV and 7.19 g L^{-1} 3-HB. Note that, in addition to a significant carbon spill in terms of acetate accumulation (15.0 g L^{-1}), there was an uncommon and relatively high-level formation of succinate and malate (up to 3.22 and 7.5 g L^{-1}, respectively) during the three feeding phases.

Strain engineering for 3-HV biosynthesis under aerobic conditions

While it is desirable to cultivate *E. coli* aerobically for effective carbon utilization and cell growth, 3-HV biosynthesis was retarded in P3HA31 under AL-III likely due to insufficient carbon diversion from succinate/succinyl-CoA node, leading to shortage of propionyl-CoA. Hence, we explored metabolic direction of dissimilated carbon flux from the TCA cycle to

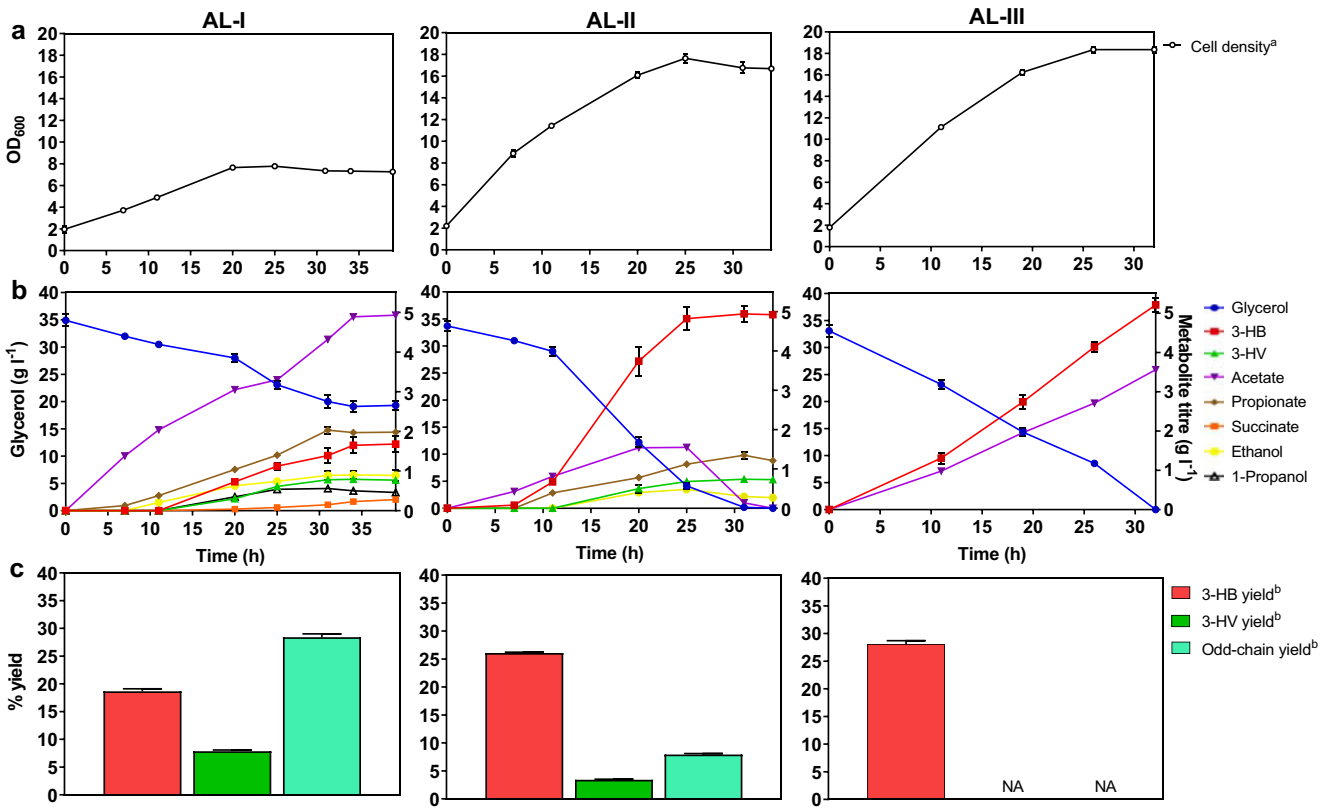

Fig. 2 Physiological effects of varying aeration levels on 3-HV production in P3HA31. Time profiles of **a** cell growth (OD_{600}), **b** glycerol consumption and metabolite production, and **c** percentage of 3-HB/3-HV/odd-chain metabolites theoretical yield based on consumed glycerol. AL-I, aeration level I; AL-II, aeration level II; and AL-III, aeration level III. Error bars represent ± SD from the mean of two replicates. [a]Measured cell density (OD_{600}) throughout cultivation period using spectrophotometer, time 0 h cell density (i.e., at the induction of IPTG) was in the range of 1.5–2.0. [b]Defined as the percentage of the 3-HB/3-HV/odd-chain metabolites theoretical yield based on the consumed glycerol. Odd-chain metabolites include 3-HV, propionate, and 1-propanol. NA, not applicable

the Sbm pathway via the glyoxylate shunt, which is metabolically active under aerobic conditions upon consumption of acetate/fatty acids (Cheng et al. 2013). To do this, we mutated *iclR* (encoding a repressor regulating the glyoxylate shunt) to derive P3HA31Δ*iclR* with a deregulated glyoxylate shunt (Fig. 5). Compared with the control strain P3HA31, P3HA31Δ*iclR* had slightly improved glycerol dissimilation and cell growth under AL-III with the production of various metabolites, including 4.44 g L^{-1} 3-HB, 0.61 g L^{-1} 3-HV, and 0.89 g L^{-1} propionate. In addition, the yield of odd-chain metabolites was approximately 7%, suggesting that the glyoxylate shunt was functional to supply succinate/succinyl-CoA as the precursor into the Sbm pathway. Interestingly, much more dissimilated carbon flux could be directed from the TCA cycle to the Sbm pathway upon combining the two mutations in the double mutant P3HA31Δ*sdhA*Δ*iclR*, significantly enhancing the production of 3-HV (1.83 g L^{-1}) and propionate (6.52 g L^{-1}) under AL-III. Note that the yield of odd-chain metabolites for P3HA31Δ*sdhA*Δ*iclR* was approximately 5-fold that for P3HA31Δ*iclR*. Also, there was hardly any carbon spill in terms of acetate secretion, implying effective carbon utilization and minimal physiological stress upon aerobic cultivation of P3HA31Δ*sdhA*Δ*iclR*. Compared with P3HA31Δ*iclR*, the increased 3-HV production occurred simultaneously with the reduced 3-HB production for P3HA31Δ*sdhA*Δ*iclR* under AL-III, suggesting that the significant carbon flux direction was associated with not only the operational glyoxylate shunt but also disrupted oxidative TCA cycle.

Fed-batch cultivation for high-level 3-HV production under aerobic conditions

To explore the full capacity of P3HA31Δ*sdhA*Δ*iclR* for 3-HV production, we conducted fed-batch cultivation under AL-III (Fig. 6). Basically, there was no further cell growth and most cells remained viable and metabolically active in all the three feeding phases. In the feeding 1 phase, the additional glycerol was effectively utilized for metabolite production with the overall yields for 3-HB, 3-HV, and odd-chain metabolites reaching 56.7%, 23.3%, and 45.5%, respectively. Interestingly, the sum of 3-HB and odd-chain metabolite yields achieved ~100%, suggesting that metabolite production was extremely effective with no carbon spill. The subsequent feeding 2 and 3 phases displayed a steady decrease in 3-HV (as well as 3-HB and propionate) production, reflected by

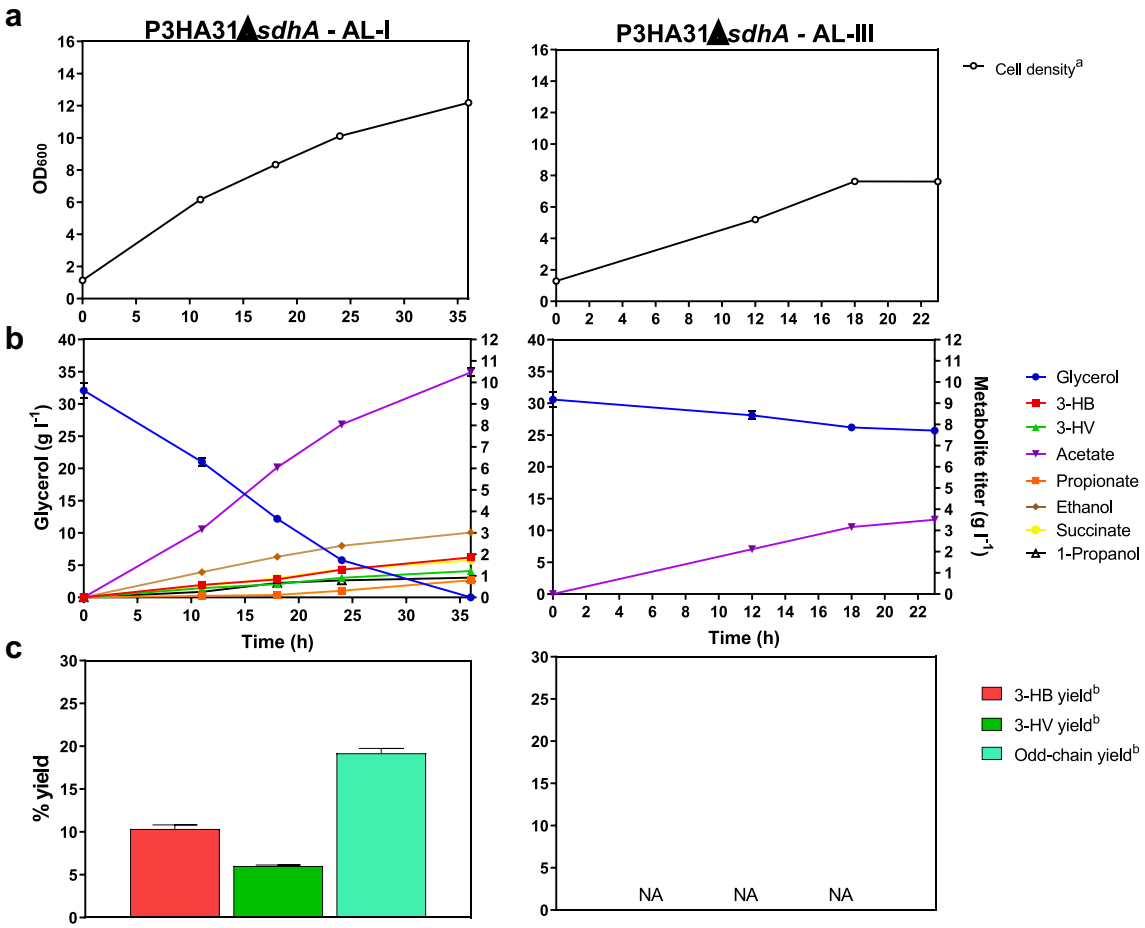

Fig. 3 Disruption of *sdhA* in P3HA31 for 3-HV production under AL-I and AL-III. Time profiles of **a** cell growth (OD_{600}), **b** glycerol consumption and metabolite production, and **c** percentage of 3-HB/3-HV/odd-chain metabolites theoretical yield based on consumed glycerol. Error bars represent ± SD from the mean of two replicates. [a]Measured cell density (OD_{600}) throughout cultivation period using spectrophotometer, time 0 h cell density (i.e., at the induction of IPTG) was in the range of 1.5–2.0. [b]Defined as the percentage of the 3-HB/3-HV/odd-chain metabolites theoretical yield based on the consumed glycerol. Odd-chain metabolites include 3-HV, propionate, and 1-propanol. NA, not applicable

monotonically decreasing 3-HV (and 3-HB and odd-chain metabolite) yields. The decreasing capacity for metabolite production occurred simultaneously with persistent acetate secretion, which started at the end of feeding 1 and reached a high level of 12.3 g L^{-1} at the end of feeding 3. Such drastic carbon spill suggested that cells experienced deteriorated physiology, limiting the overall cultivation performance. Nevertheless, the final 3-HV, 3-HB, and propionate titers of the fed-batch cultivation under AL-III reached 7.3 g L^{-1}, 11.3 g L^{-1}, and 11.9 g L^{-1}, respectively. To reduce acetate secretion, we conducted another similar fed-batch cultivation by increasing the air flowrate into the bulk culture to 2 vvm during the initial batch stage and then to 4 vvm during the three feeding phases (AL-IV) (Fig. 7). The initial batch stages for the two fed-batch cultures under AL-III and AL-IV behaved similarly in cell growth and metabolite production. However, as opposed to the AL-III fed-batch culture, cell density further increased in the feeding 1 phase under a higher aeration rate of AL-IV. The glycerol dissimilation rate during the three feeding phases also increased under AL-IV, reducing the overall cultivation time from 118 to 98 h. Most importantly, the production of key metabolites significantly improved with a much reduced carbon spill. The most effective metabolite production period occurred in the feeding 2 phase, with the overall yields for 3-HB, 3-HV, and odd-chain metabolites reaching 43.4%, 36.5%, and 54.7%, respectively. Note that the sum of 3-HB and odd-chain metabolite yields also achieved ~ 100%. Compared with the AL-III fed-batch culture, the onset of acetate secretion of the AL-IV fed-batch culture was delayed to the early feeding 2 phase and acetate reached a lower level of 8.1 g L^{-1} at the end of feeding 3. The final 3-HV, 3-HB, and propionate titers of the AL-IV fed-batch culture reached high levels of 10.6 g L^{-1}, 11.3 g L^{-1}, and 12.7 g L^{-1}, equivalent to overall yields of 18.8%, 22.8%, and 18.1%, respectively. To the best of our knowledge, the current report represents the most effective bio-based

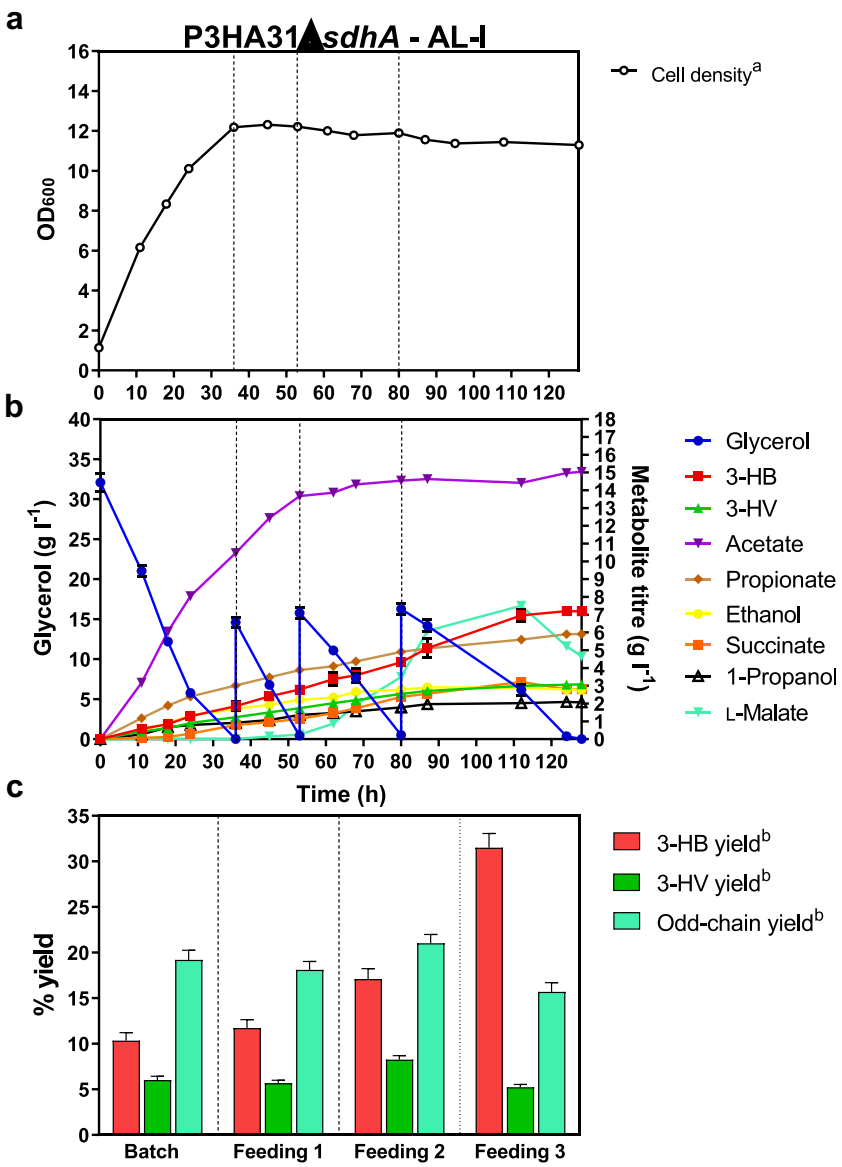

Fig. 4 Fed-batch cultivation of P3HA31Δ*sdhA* under extended AL-I conditions. Time profiles of **a** cell growth (OD_{600}), **b** glycerol consumption and metabolite production, and **c** percentage of 3-HB/3-HV/odd-chain metabolites theoretical yield based on consumed glycerol during each feeding phase. Dotted vertical lines in panels **a** and **b** separate batch, feeding 1, feeding 2, and feeding 3 stages of fermentation. Error bars represent ± SD from the mean of two replicates. [a]Measured cell density (OD_{600}) throughout cultivation period using spectrophotometer, time 0 h cell density (i.e., at the induction of IPTG) was in the range of 1.5–2.0. [b]Defined as the percentage of the 3-HB/3-HV/odd-chain metabolites theoretical yield based on the consumed glycerol. Odd-chain metabolites include 3-HV and propionate

production of 3-HV to date using structurally unrelated carbon sources.

Discussion

Several physiological and metabolic factors can potentially affect 3-HV production, including cell growth (and glycerol dissimilation), intracellular abundance of propionyl-CoA as a key precursor, and metabolic activity of the hydroxyacid biosynthetic pathway. Our results suggest that the first two, but not the third one, were highly sensitive to the oxygenic condition of the culture. While the Sbm fermentation was favored by anaerobiosis, reflected by a higher odd-chain yield for P3HA31 under AL-I than that under AL-II or AL-III, the low oxygenic level retarded cell growth, resulting in a high carbon spill. The acetate accumulation could also limit carbon flux toward the reductive TCA branch at the PEP node (Fig. 1), which was identified as the major route for dissimilated carbon being directed toward the Sbm pathway (Srirangan et al. 2016b). The two issues of retarded cell growth and high acetate secretion were simultaneously resolved upon marginally increasing the oxygenic level through cultivation of P3HA31 under AL-II. However, the resolution was at the expense of a reduced propionyl-CoA level, reflected by significantly lower 3-HV and odd-chain yields for the AL-II culture, compared with the AL-I culture. Further increasing the oxygenic level upon cultivation of P3HA31 under AL-III abolished the production of 3-HV and other odd-chain metabolites though cell growth was effective, implying that more dissimilated carbon flux upon glycolysis was directed toward the acetyl-CoA node rather than the PEP

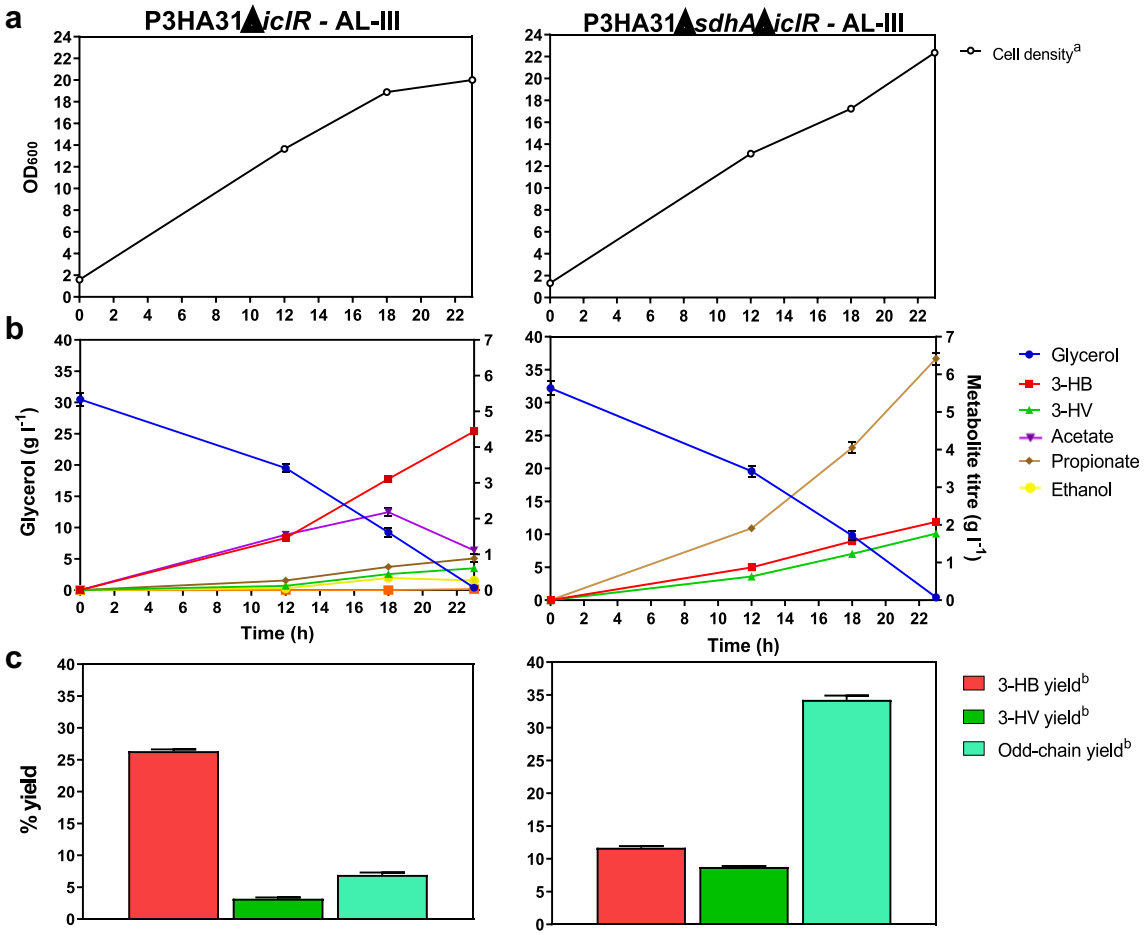

Fig. 5 Comparing the effects of P3HA31Δ*iclR* and P3HA31Δ*sdhA*Δ*iclR* for 3-HV production under AL-III conditions. Time profiles of **a** cell growth (OD_{600}), **b** glycerol consumption and metabolite production, and **c** percentage of 3-HB/3-HV/odd-chain metabolites theoretical yield based on consumed glycerol. Error bars represent ± SD from the mean of two replicates. [a]Measured cell density (OD_{600}) throughout cultivation period using spectrophotometer, time 0 h cell density (i.e., at the induction of IPTG) was in the range of 1.5–2.0. [b]Defined as the percentage of the 3-HB/3-HV/odd-chain metabolites theoretical yield based on the consumed glycerol. Odd-chain metabolites include 3-HV and propionate

node into the reductive TCA branch. Consistently, acetate accumulated more under AL-III potentially due to an increased level of acetyl-CoA. On the other hand, the metabolic activity of 3-hydroxyacid biosynthetic pathway was minimally affected by the oxygenic condition as the sums of the overall 3-HV and 3-HB yields were approximately the same for the three P3HA31 cultures, i.e., 27.0%, 29.5%, and 28.1% for AL-I, AL-II, and AL-III, respectively (Fig. 2), suggesting that 3-hydroxyacids can be effectively produced under both aerobic and anaerobic conditions.

As succinate (and, therefore, succinyl-CoA) is a key precursor predating the Sbm pathway, the level of the Sbm fermentation can depend on the supply of succinate. Intracellular formation of succinate can be achieved via three oxygen-dependent pathways, i.e., (i) reductive TCA branch (i.e., reverse TCA cycle), (ii) oxidative TCA cycle, and (iii) glyoxylate shunt (Cheng et al. 2013). Normally, succinate accumulates as an end-product of mixed acid fermentation in *E. coli* via the reductive TCA branch which is activated under anaerobic conditions (Cheng et al. 2013; Thakker et al. 2012). Although the reductive TCA branch can potentially yield high-level succinate, its metabolic activity for biosynthesis is often limited by the availability of reducing equivalents (i.e., NADH) (Skorokhodova et al. 2015). Under aerobic conditions, succinate is normally used up as an intermediate of the oxidative TCA cycle without accumulation, except for the conditions of oxidative stress and/or acetate/fatty-acid consumption under which succinate can be aerobically derived via an operational glyoxylate shunt (Cheng et al. 2013; Thakker et al. 2012). Glyoxylate shunt can provide anaplerotic reactions and bypass the CO_2-producing steps in the oxidative TCA cycle, thereby conserving carbon atoms for the cell (Gottschalk 1986; Kornberg and Madsen 1957). Given that succinate is involved in the central metabolism, manipulation of carbon flux around this C4-dicarboxylate can be challenging due to high oxygen sensitivity for its

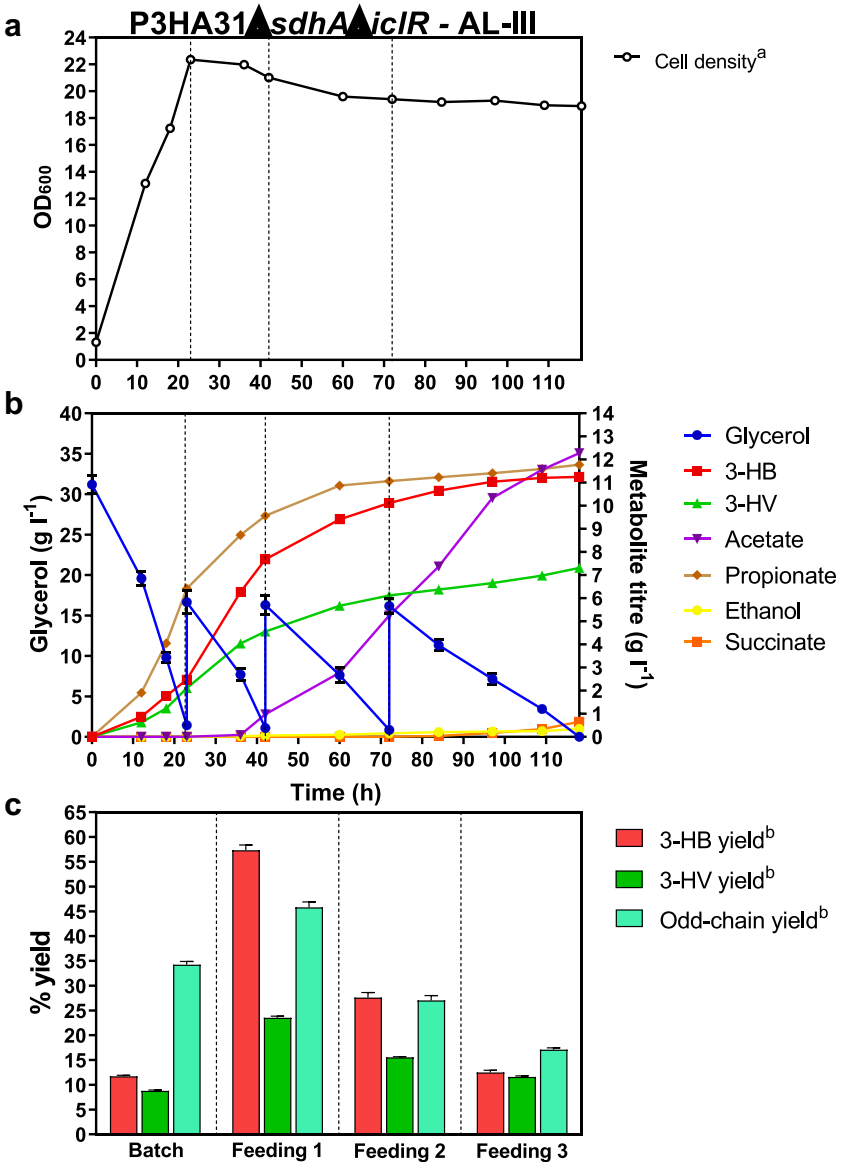

Fig. 6 Fed-batch cultivation of P3HA31Δ*sdhA*Δ*iclR* under extended AL-III conditions. Time profiles of **a** cell growth (OD_{600}), **b** glycerol consumption and metabolite production, and **c** percentage of 3-HB/3-HV/odd-chain metabolites theoretical yield based on consumed glycerol during each feeding phase. Dotted vertical lines in panels **a** and **b** separate batch, feeding 1, feeding 2, and feeding 3 stages of fermentation. Error bars represent ± SD from the mean of two replicates. [a]Measured cell density (OD_{600}) throughout cultivation period using spectrophotometer, time 0 h cell density (i.e., at the induction of IPTG) was in the range of 1.5–2.0 [b]Defined as the percentage of the 3-HB/3-HV/odd-chain metabolites theoretical yield based on the consumed glycerol. Odd-chain metabolites include 3-HV and propionate

production. Therefore, proper operation of the TCA cycle can effectively direct dissimilated carbon flux toward the Sbm pathway to form propionyl-CoA.

By inactivating the oxidative TCA cycle in P3HA31Δ*sdhA* under microaerobic conditions, more dissimilated carbon flux could be channeled to the Sbm pathway via the reductive TCA branch to form propionyl-CoA. While cell growth and 3-HV biosynthesis under microaerobic conditions were enhanced compared with the control strain P3HA31, significant carbon spill still existed in P3HA31Δ*sdhA* particularly during fed-batch cultivation. Such unfavorable culture conditions even resulted in uncommon and significant accumulation of TCA metabolites of malate and succinate, potentially associated with reduced enzyme activities of FumB and SucCD in the reductive TCA branch and, consequently, limited the carbon flux channeling to the Sbm pathway.

Under aerobic conditions such as AL-III, the control strain P3HA31 primarily operated the oxidative TCA cycle for respiration. Thus, inactivating the TCA oxidative cycle in P3HA31Δ*sdhA* under AL-III significantly retarded cell growth with limited glycerol dissimilation and metabolite production. Substantial inhibition of the TCA cycle under a high oxygen exposure was previously observed upon disruption of the succinate dehydrogenase complex in *E. coli*, resulting in reduced supply of NADH to the aerobic respiratory chain, and thus diminished cell growth/metabolic activity (Guest 1981; Steinsiek et al. 2011). Glyoxylate shunt could serve as an alternative route to drive the TCA cycle under aerobic conditions (Nègre et al. 1992; Sunnarborg et al. 1990), and deregulation of the glyoxylate shunt via the *iclR* mutation in P3HA31 could potentially enhance the metabolic activity of this pathway, resulting in not only vigorous cell growth but

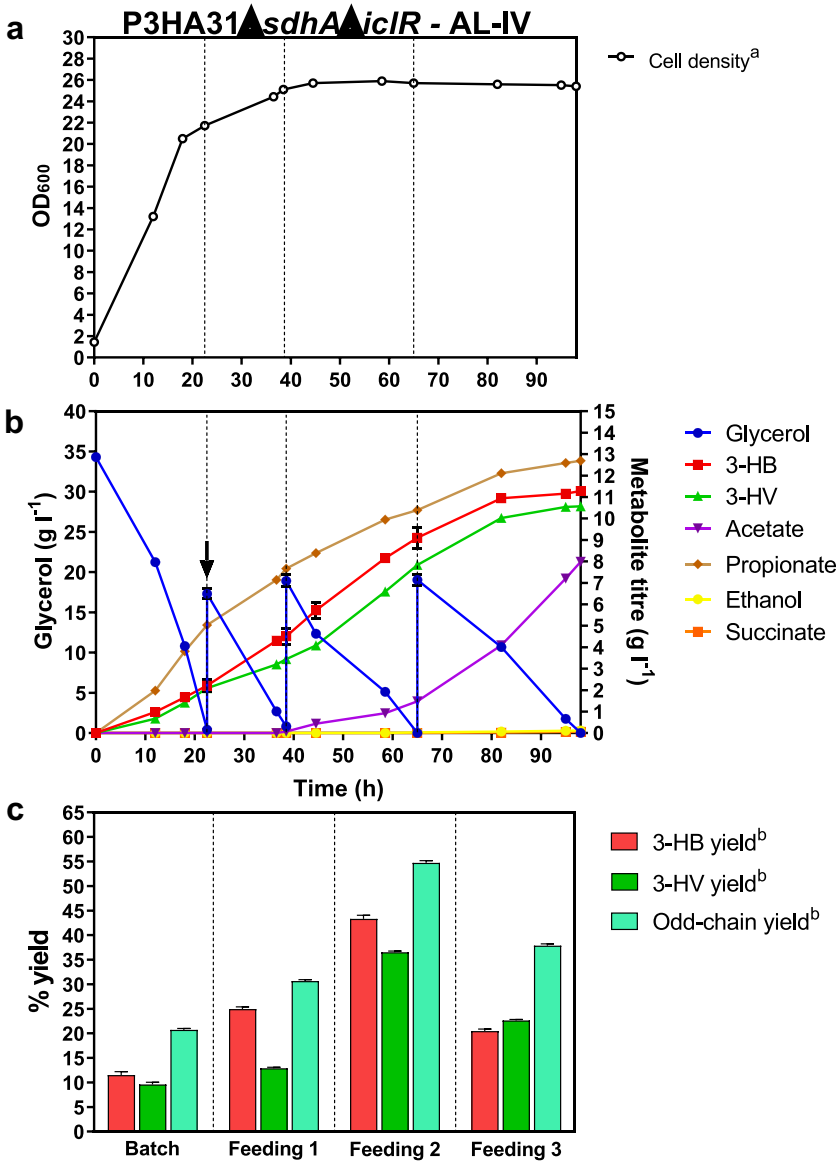

Fig. 7 Fed-batch cultivation of P3HA31Δ*sdhA*Δ*iclR* under AL-IV conditions. Time profiles of **a** cell growth (OD_{600}), **b** glycerol consumption and metabolite production, and **c** percentage of 3-HB/3-HV/odd-chain metabolites theoretical yield based on consumed glycerol during each feeding phase. Dotted vertical lines in panels **a** and **b** separate batch, feeding 1, feeding 2, and feeding 3 stages of fermentation. Black arrow indicates the point of airflow switch from 2 vvm to 4 vvm. Error bars represent ± SD from the mean of two replicates. [a]Measured cell density (OD_{600}) throughout cultivation period using spectrophotometer, time 0 h cell density (i.e., at the induction of IPTG) was in the range of 1.5–2.0. [b]Defined as the percentage of the 3-HB/3-HV/odd-chain metabolites theoretical yield based on the consumed glycerol. Odd-chain metabolites include 3-HV and propionate

also metabolite biosynthesis. Note that the final 3-HB and 3-HV titers for P3HA31Δ*iclR* went up to 4.44 and 0.61 g L^{-1}, respectively, equivalent to 26.3% and 3.2% yields, suggesting that 3-hydroxyacid biosynthesis was quite active under AL-III. The production of propionate and 3-HV, though with a decent overall odd-chain yield of 6.9%, suggested that the Sbm pathway was active in P3HA31Δ*iclR* under AL-III. In comparison to higher odd-chain yields obtained under more anaerobic conditions, the relatively low odd-chain yield for P3HA31Δ*iclR* under AL-III was primarily associated with the active TCA oxidative cycle, which caused a carbon flux diversion at the succinate node. Importantly, the flux diversion could be prevented with enhanced production of the odd-chain metabolites by simultaneous knockout of *sdhA* and *iclR* in P3HA31. Up to 6.52 g L^{-1} propionate and 1.83 g L^{-1} 3-HV, equivalent to an overall odd-chain yield at 35.0%, were produced in P3HA31Δ*sdhA*Δ*iclR* under AL-III, suggesting that more dissimilated carbon flux was successfully directed from the TCA cycle to the Sbm pathway. Such carbon flux channeling hardly occurred when the oxidative TCA branch was functional, resulting in no production of odd-chain metabolites in the control strain P3HA31 under AL-III. The severely retarded glycerol dissimilation and cell growth for P3HA31Δ*sdhA* could be complemented by the *iclR* mutation, suggesting that both the oxidative TCA cycle and glyoxylate shunt contributed to active TCA operation for sustained cell growth under AL-III. Our results also suggested that the dissimilated carbon flux was directed from the TCA cycle to the Sbm pathway via glyoxylate shunt and reductive TCA branch rather than oxidative TCA branch. Furthermore, the sum of 3-HB and 3-HV yields was somewhat lower in P3HA31Δ*sdhA*Δ*iclR* (21.3%) than P3HA31Δ*iclR* (29.5%),

and such reduction was primarily associated with an effective propionate production in P3HA31Δ*sdhA*Δ*iclR* than reduced 3-hydroxyacid biosynthesis. Finally, it is noteworthy that the secreted acetate could be dissimilated in P3HA31Δ*iclR* toward the end of batch cultivation and acetate was not even secreted in P3HA31Δ*sdhA*Δ*iclR*, suggesting that the enhanced glyoxylate shunt with a disrupted oxidative TCA cycle could facilitate not only acetyl-CoA utilization, thereby reducing carbon spill, but also carbon direction from the TCA cycle to the Sbm pathway for biosynthesis of odd-chain metabolites. As the Sbm fermentation still occurred under AL-III for P3HA31Δ*sdhA*Δ*iclR*, the lack of 3-HV production in the control strain P3HA31 under AL-III was primarily associated with the shortage of succinate precursor and inactive glyoxylate shunt for the carbon flux direction.

Using the engineered strain P3HA31Δ*sdhA*Δ*iclR*, we further demonstrated its high capacity for producing both 3-HV and 3-HB through fed-batch cultivation under aerobic conditions of AL-III and AL-IV. In particular, during certain feeding stages, such as feeding 1 under AL-III and feeding 2 under AL-IV, metabolite production was extremely effective with no carbon spill, and a total 3-hydroxyacid yield of ~80% was achieved. It is worth highlighting that the metabolite-producing capacity was actively maintained throughout most of the three feeding phases of both fed-batch cultures. Nevertheless, 3-hydroxyacid production was limited by carbon spill toward acetogenesis particularly during the feeding 2 and 3 phases in the AL-III fed-batch culture, resulting in high-level acetate secretion. Such carbon spill was shown to be associated with oxygen limitation since increasing the aeration rate in the AL-IV fed-batch culture could significantly reduce acetate secretion with enhanced 3-HV production. It was previously reported that increasing the culture aerobicity can potentially enable cells to recycle accumulated acetyl-CoA (thereby reduce acetate formation) for biosynthesis through enhanced glyoxylate shunt, which involves acetyl-CoA as a co-substrate and is typically active under aerobic conditions (Ahn et al. 2016; Renilla et al. 2012). Nevertheless, complete elimination of acetate during aerobic growth of *E. coli* can be a rather difficult task due to physiological challenges of overflow metabolism (data not shown).

In summary, our results suggest that the Sbm pathway can be metabolically active under both anaerobic and aerobic conditions for 3-HV to be produced. In addition, the production of 3-HV (and other odd-chain metabolites derived from propionyl-CoA) can be critically limited by the level of the dissimilated carbon flux directed from the TCA cycle to the Sbm pathway, and such carbon flux direction can be enhanced by manipulation of key TCA genes (i.e., *sdhA* and *iclR*) in the 3-HV-producing cell and proper control of the oxygenic condition in the bacterial culture.

Author contributions DM conceived the study, formulated research plan, coordinated research team, carried out experiments, performed result interpretation and data analysis, and drafted the manuscript. JM, TK, DA, and CH helped to carry out experiments and data analysis. MMY and CPC conceived, planned, supervised, and managed the study, as well as helped to draft the manuscript. All authors read and approved the final manuscript.

Funding information This work was supported by the following Government of Canada grants: (1) Natural Sciences and Engineering Research Council (NSERC) Strategic Partnership grant 430106-12; (2) Canada Research Chair (CRC) grant 950-211471; and (3) Networks of Centres of Excellence of Canada (BioFuelNet Canada (BFN)).

Compliance with ethical standards

Conflict of interest The authors declare that they have no competing interests.

Ethical approval This article does not contain any studies with human participants or animals performed by any of the authors.

References

Ahn S, Jung J, Jang I-A, Madsen EL, Park W (2016) Role of glyoxylate shunt in oxidative stress response. J Biol Chem 291(22):11928–11938

Akawi L, Srirangan K, Liu X, Moo-Young M, Chou CP (2015) Engineering *Escherichia coli* for high-level production of propionate. J Ind Microbiol Biot 42(7):1057–1072

Amann E, Ochs B, Abel K-J (1988) Tightly regulated *tac* promoter vectors useful for the expression of unfused and fused proteins in *Escherichia coli*. Gene 69(2):301–315

Anis SNS, Mohamad Annuar MS, Simarani K (2017) In vivo and in vitro depolymerizations of intracellular medium-chain-length poly-3-hydroxyalkanoates produced by *Pseudomonas putida* Bet001. Prep Biochem Biotech 47(8):824–834

Baba T, Ara T, Hasegawa M, Takai Y, Okumura Y, Baba M, Datsenko KA, Tomita M, Wanner BL, Mori H (2006) Construction of *Escherichia coli* K-12 in-frame, single-gene knockout mutants: the Keio collection. Mol Syst Biol 2:1–11

Biernacki M, Riechen J, Hähnel U, Roick T, Baronian K, Bode R, Kunze G (2017) Production of (*R*)-3-hydroxybutyric acid by *Arxula adeninivorans*. AMB Express 7(1):4–16

Cheng K-K, Wang G-Y, Zeng J, Zhang J-A (2013) Improved succinate production by metabolic engineering. Biomed Res Int 2013:1–12

Cherepanov PP, Wackernagel W (1995) Gene disruption in *Escherichia coli*: TcR and KmR cassettes with the option of Flp-catalyzed excision of the antibiotic-resistance determinant. Gene 158(1):9–14

Ciriminna R, Pina CD, Rossi M, Pagliaro M (2014) Understanding the glycerol market. Eur J Lipid Sci Tech 116(10):1432–1439

Datsenko KA, Wanner BL (2000) One-step inactivation of chromosomal genes in *Escherichia coli* K-12 using PCR products. PNAS 97(12):6640–6645

de Roo G, Kellerhals MB, Ren Q, Witholt B, Kessler B (2002) Production of chiral *R*-3-hydroxyalkanoic acids and *R*-3-hydroxyalkanoic acid methylesters via hydrolytic degradation of polyhydroxyalkanoate synthesized by pseudomonads. Biotechnol Bioeng 77(6):717–722

Fonseca AC, Lima MS, Sousa AF, Silvestre AJ, Coelho JFJ, Serra AC (2019) Cinnamic acid derivatives as promising building blocks for

advanced polymers: synthesis, properties and applications. Polym Chem 10(14):1696–1723
Gibson DG, Young L, Chuang R-Y, Venter JC, Hutchison CA, Smith HO (2009) Enzymatic assembly of DNA molecules up to several hundred kilobases. Nat Methods 6(5):343–345
Gottschalk G (1986) Bacterial metabolism. Springer, New York
Guest JR (1981) Partial replacement of succinate dehydrogenase function by phage- and plasmid-specified fumarate reductase in *Escherichia coli*. J Gen Microbiol 122(2):171–179
Huang PQ, Ye JL, Chen Z, Ruan YP, Gao JX (1998) A versatile approach to the activated form of (3*S*, 4*R*)-Statine and its analogues. Synth Commun 28(3):417–426
Jobling MG, Holmes RK (1990) Construction of vectors with the pl5a replicon, kanamycin resistance, inducible lacZα and pUC18 or pUC19 multiple cloning sites. Nucleic Acids Res 18(17):5315–5315
Kaur G, Roy I (2015) Strategies for large-scale production of polyhydroxyalkanoates. Chem Biochem Eng Q 29(2):157–172
Kornberg H, Madsen N (1957) Synthesis of C4-dicarboxylic acids from acetate by a "glyoxylate bypass" of the tricarboxylic acid cycle. Biochim Biophys Acta 24:651–653
Lau NS, Ch'ng DE, Chia KH, Wong YM, Sudesh K (2014) Advances in polyhydroxyalkanoate (PHA): unraveling the development and new perspectives. J Biobased Mater Bioenergy 9(2):118–129
Luo RC, Wu YL, i-Newehy M (2014) The industrial production of PHA. In: Polyhydroxyalkanoates (PHAs): biosynthesis, industrial production and applications in medicine, p 133-139
Mao Y, Li G, Chang Z, Tao R, Cui Z, Wang Z, Tang Y-J, Chen T, Zhao X (2018) Metabolic engineering of *Corynebacterium glutamicum* for efficient production of succinate from lignocellulosic hydrolysate. Biotechnol Biofuels 11(1):95–112
Martin CH, Prather KLJ (2009) High-titer production of monomeric hydroxyvalerates from levulinic acid in *Pseudomonas putida*. J Biotechnol 139(1):61–67
Miller JH (1992) A short course in bacterial genetics: a laboratory manual and handbook for *Escherichia coli* and related bacteria. Cold Spring Harbor Laboratory Press, NY
Miscevic D, Srirangan K, Kefale T, Kilpatrick S, Chung DA, Moo-Young M, Chou CP (2019) Heterologous production of 3-hydroxyvalerate in engineered *Escherichia coli*. Metab Eng In-press
Mori K (1981) A simple synthesis of (*S*)-(+)-sulcatol, the pheromone of *Gnathotrichus retusus*, employing baker's yeast for asymmetric reduction. Tetrahedron 37(7):1341–1342
Murarka A, Dharmadi Y, Yazdani SS, Gonzalez R (2008) Fermentative utilization of glycerol by *Escherichia coli* and its implications for the production of fuels and chemicals. Appl Environ Microbiol 74(4): 1124–1135
Nahar L, Turner AB, Sarker SD (2009) Synthesis of hydroxy acids of dinorcholane and 5^2-cholane. J Brazil Chem Soc 20:88–92
Nègre D, Cortay J-C, Galinier A, Sauve P, Cozzone AJ (1992) Specific interactions between the IclR repressor of the acetate operon of *Escherichia coli* and its operator. J Mol Biol 228(1):23–29
Neidhardt FC, Bloch PL, Smith DF (1974) Culture medium for Enterobacteria. J Bacteriol 119(3):736–747
Noyori R, Kitamura M, Ohkuma T (2004) Toward efficient asymmetric hydrogenation: architectural and functional engineering of chiral molecular catalysts. PNAS 101(15):5356–5362
Ren Q, Ruth K, Thöny-Meyer L, Zinn M (2010) Enatiomerically pure hydroxycarboxylic acids: current approaches and future perspectives. Appl Microbiol Biotechnol 87(1):41–52
Renilla S, Bernal V, Fuhrer T, Castaño-Cerezo S, Pastor JM, Iborra JL, Sauer U, Cánovas M (2012) Acetate scavenging activity in *Escherichia coli*: interplay of acetyl–CoA synthetase and the PEP–glyoxylate cycle in chemostat cultures. Appl Microbiol Biotechnol 93(5):2109–2124
Skorokhodova AY, Morzhakova AA, Gulevich AY, Debabov VG (2015) Manipulating pyruvate to acetyl-CoA conversion in *Escherichia coli* for anaerobic succinate biosynthesis from glucose with the yield close to the stoichiometric maximum. J Biotechnol 214:33–42
Snell KD, Peoples OP (2009) PHA bioplastic: a value-added coproduct for biomass biorefineries. Biofuels Bioprod Biorefin 3(4):456–467
Spengler J, Albericio F (2014) ChemInform abstract: asymmetric synthesis of α-unsubstituted β-hydroxy acids. ChemInform 45(30):151–161
Srirangan K, Akawi L, Liu X, Westbrook A, Blondeel EJ, Aucoin MG, Moo-Young M, Chou CP (2013) Manipulating the sleeping beauty mutase operon for the production of 1-propanol in engineered *Escherichia coli*. Biotechnol Biofuels 6(1):1–14
Srirangan K, Liu X, Westbrook A, Akawi L, Pyne ME, Moo-Young M, Chou CP (2014) Biochemical, genetic, and metabolic engineering strategies to enhance coproduction of 1-propanol and ethanol in engineered *Escherichia coli*. Appl Microbiol Biotechnol 98(22): 9499–9515
Srirangan K, Liu X, Akawi L, Bruder M, Moo-Young M, Chou CP (2016a) Engineering *Escherichia coli* for microbial production of butanone. Appl Environ Microbiol 82:2574–2584
Srirangan K, Liu X, Tran TT, Charles TC, Moo-Young M, Chou C, P. (2016b) Engineering of *Escherichia coli* for direct and modulated biosynthesis of poly(3-hydroxybutyrate-*co*-3-hydroxyvalerate) copolymer using unrelated carbon sources. Sci Rep 6:36470
Steinsiek S, Frixel S, Stagge S, Bettenbrock K (2011) Characterization of *E. coli* MG1655 and *frdA* and *sdhC* mutants at various aerobiosis levels. J Biotechnol 154(1):35–45
Sunnarborg A, Klumpp D, Chung T, LaPorte DC (1990) Regulation of the glyoxylate bypass operon: cloning and characterization of *iclR*. J Biotechnol 172(5):2642–2649
Taroncher-Oldenburg G, Nishina K, Stephanopoulos G (2000) Identification and analysis of the polyhydroxyalkanoate-specific β-ketothiolase and acetoacetyl coenzyme a reductase genes in the *Cyanobacterium Synechocystis* sp. strain PCC6803. Appl Environ Microbiol 66(10):4440–4448
Thakker C, Martínez I, San K-Y, Bennett GN (2012) Succinate production in *Escherichia coli*. Biotechnol J 7(2):213–224
Toshiyuki C, Takeshi N (1987) A new synthetic approach to the carbapenem antibiotic PS-5 from ethyl (*S*)-3-hydroxybutanoate. Chem Lett 16(11):2187–2188
Tseng H-C, Martin CH, Nielsen DR, Prather KLJ (2009) Metabolic engineering of *Escherichia coli* for enhanced production of (*R*)- and (*S*)-3-hydroxybutyrate. Appl Environ Microbiol 75(10):3137–3145
Tseng H-C, Harwell CL, Martin CH, Prather KL (2010) Biosynthesis of chiral 3-hydroxyvalerate from single propionate-unrelated carbon sources in metabolically engineered *E. coli*. Microb Cell Factories 9(1):1–12
Xu J, Han M, Zhang J, Guo Y, Qian H, Zhang W (2014) Improvement of L-lysine production combines with minimization of by-products synthesis in *Corynebacterium glutamicum*. J Chem Technol Biot 89(12):1924–1933
Yaguchi A, Spagnuolo M, Blenner M (2018) Engineering yeast for utilization of alternative feedstocks. Curr Opin Biotech 53:122–129
Yazdani SS, Gonzalez R (2007) Anaerobic fermentation of glycerol: a path to economic viability for the biofuels industry. Curr Opin Biotech 18(3):213–219
Zhou X, Ye L, Wu JC (2013) Efficient production of l-lactic acid by newly isolated thermophilic *Bacillus coagulans* WCP10-4 with high glucose tolerance. Appl Microbiol Biotechnol 97(10):4309–4314
Zhu C, Chiu S, Nakas JP, Nomura CT (2013) Bioplastics from waste glycerol derived from biodiesel industry. J Appl Polym Sci 130(1): 1–13